Wind and Structures, Vol. 1, No. 3 (1998) 255-269
DOI: http://dx.doi.org/10.12989/was.1998.1.3.255

Moment-curvature relationships to estimate deflections and second-order moments in wind-loaded RC chimneys and towers

Devdas Menon†

Department of Civil Engineering, Indian Institute of Technology, Madras, 600-036, India

Abstract. Second-order moments of considerable magnitude arise in tall and slender RC chimneys and towers subject to along-wind loading, on account of eccentricities in the distributed self-weight of the tower in the deflected profile. An accurate solution to this problem of *geometric nonlinearity* is rendered difficult by the uncertainties in estimating the flexural rigidity of the tower, due to variable cracking of concrete and the 'tension stiffening' effect. This paper presents a rigorous procedure for estimating deflections and second-order moments in wind-loaded RC tubular towers. The procedure is essentially based on a generalised formulation of moment-curvature relationships for RC tubular towers, derived from the experimental and theoretical studies reported by Schlaich *et al.* 1979 and Menon 1994 respectively. The paper also demonstrates the application of the proposed procedure, and highlights those conditions wherein second-order moments become too significant to be overlooked in design.

Key words: reinforced concrete; chimneys; towers; moment-curvature relationship; tension stiffening effect; second-order moment; geometric nonlinearity; along-wind response.

1. Introduction

Tall reinforced concrete (RC) towers are widely used, in increasing numbers and increasing heights, for various applications, such as industrial chimneys and towers for TV transmission and microwave communication. Such towers are typically hollow circular in cross-section, from aerodynamic considerations, and tapered along their heights, from considerations of structural economy and aesthetics. Wind loads generally predominate the structural proportioning of the tower, which behaves essentially as a vertical cantilever, and is usually analysed in practice without significant error using conventional beam elements (Menon and Reddy 1998). The tubular section of the vertical shaft is typically subjected to a bending moment due to lateral wind load, combined with an axial compression due to the dead load of the tower above the section under consideration. Simplified methods of estimating the design bending moments due to dynamic wind action, in the along-wind as well as across-wind directions, have been recommended in various international codes of practice on RC chimney design. A comparative study of these methods for estimating along-wind moments is described in Menon and Rao 1997a; methods for estimating across-wind moments are reviewed in Menon and Rao 1997b. Also, an assessment of the reliabilities, in terms of lifetime probabilities of

† Assistant Professor

failure, associated with the various codal methods of design, is given in Menon and Rao 1998.

Wind moments in towers are usually computed in design practice, on the basis of a dynamic or quasi-static analysis, which assumes *linear elastic* behaviour. However, in reality, the behaviour is *nonlinear*; i.e., the deflections increase nonlinearly with increase in wind loading, especially in the along-wind direction. There is a problem of *geometric nonlinearity*, whereby 'second-order moments' are induced, on account of eccentricities in the distributed self-weight of the tower in the deflected profile. There is also a problem of *material nonlinearity*, triggered by the cracking of concrete, causing variations in flexural stiffness and damping ratios. These effects introduce uncertainties that make the prediction of deflections and second-order moments a difficult task. Consequently, many code-based methods (ACI 307, 1988, DIN 1056 1984, Pinfold 1984) do not require second-order moments to be computed by the designer; these are accounted for by means of a conservative selection of safety factors. The ACI code, for example, accommodates these additional moments by lowering the *resistance factor*, as stated in the Commentary to the code (ACI 307 1988). However, a few chimney codes (IS 4998, 1992, CICIND 1984) do require these moments to be computed explicitly, although no rigorous procedure is specified. The CICIND Model Chimney Code, however, does give a simplified formula to facilitate a rough estimate.

Some experimental studies on RC hollow circular sections have been reported in literature (Schlaich *et al.* 1979, Mokrin and Rumman 1985). Simplified theoretical procedures (Naokowski 1981, Naokowski and Gerstle 1990) have also been formulated to enable the prediction of second-order moments in RC chimneys (of cylindrical shape), although it is not clear whether these proposals have the support of experimental evidence.

The work reported here is a contribution in this area. A rigorous procedure for estimating deflections and second-order moments in wind-loaded RC tubular towers (of all shapes) is presented here. The procedure is essentially based on a generalised formulation of moment-curvature relationships for RC tubular towers, derived from the experimental and theoretical studies reported by Schlaich *et al.* 1979 and Menon 1994 respectively. The paper also demonstrates the application of the proposed procedure, and highlights those conditions wherein second-order moments become too significant to be overlooked in design.

2. Difficulties in accurate prediction of deflections

Deflections in RC members are, in general, difficult to predict with accuracy. The calculations are usually considered in two parts: (i) immediate or short-term deflection and (ii) additional long-term deflection due to creep and shrinkage. In the present context of deflections of RC towers under wind load, we may conveniently ignore the second (and more difficult) component of long-term deflection. However, even short-term deflections in normal RC members are not easy to predict, mainly due to uncertainties in the estimation of *flexural rigidity*, which is influenced by :

- varying degrees of tensile cracking in concrete;
- varying amounts of reinforcement;
- presence of axial forces, in addition to flexure;
- variations in the tensile strength of concrete;
- variations in the modulus of elasticity of concrete;
- nonlinear stress-strain curve of concrete in compression.

In addition, there is an inherent high variability in measured deflections, even under carefully controlled laboratory conditions.

Despite the above uncertainties, a number of simplified procedures have been developed over the years, and incorporated in codes, to estimate short-term deflections in RC beams. These procedures adopt empirical expressions for estimating the so-called 'effective flexural rigidity' (Branson 1977, Yu and Winter 1960, Beeby and Miles 1969, Rao and Subrahmanyam 1973, Prakhya and Morely, 1990). The influence of axial force, in combination with flexure, has also been accounted for by Sakai and Kakuta, 1980.

However, these well-known procedures to predict short-term deflections in RC members in general (for the purpose of ensuring satisfactory *serviceability* performance) cannot be readily applied to the case of determining deflections and second-order moments in wind-loaded RC towers, for the following reasons :

- The assumption of linear elastic behaviour, underlying the conventional procedures, is justifiable under *service load* conditions, but surely not under *extreme wind* conditions. The effect of nonlinearities must be properly accounted for in the estimation of second-order moments for a realistic assessment of ultimate moments in limit state (strength) design (Menon 1994).
- The behaviour of concrete in RC flexural members with very large hollow circular cross-sections is different from conventional RC beams with relatively small and solid cross-sections. In the case of the former (unlike the latter), the distribution of compressive stresses is more-or-less uniform across the local thickness of the concrete shell (Rao and Menon 1995).

3. Moment-curvature relationships in tubular RC sections

Experimental studies (Schlaich *et al.* 1979) on tubular RC beam specimens, subjected to uniform increasing bending moment (M), combined with constant axial compression (N), indicate that the overall shape of the moment-curvature (M-φ) plot is similar to that obtainable for conventional RC beam specimens. The shape of the typical M-φ curve is

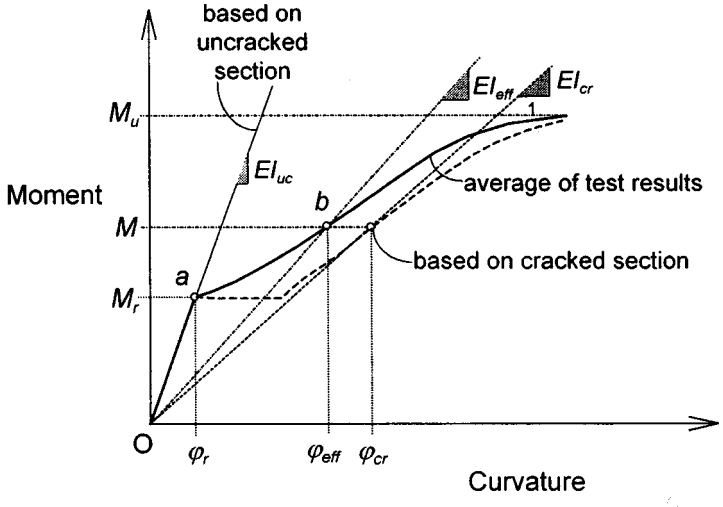

Fig. 1 Typical moment-curvature relationships for tubular RC sections

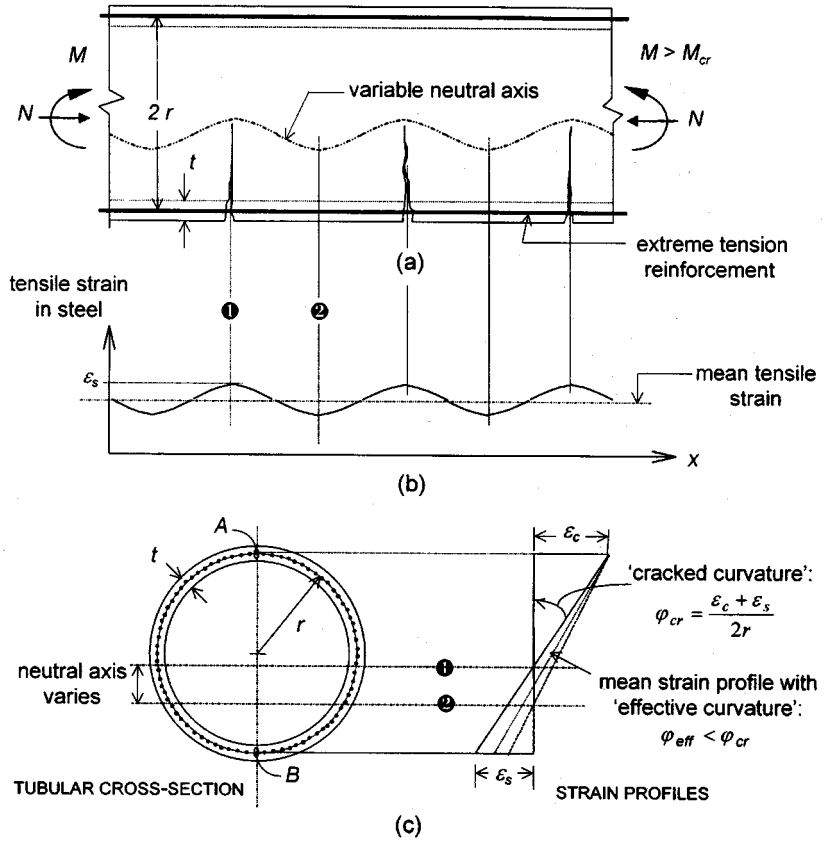

Fig. 2 Effect of cracking in a tubular RC beam subject to uniform moment (M) and axial compression (N)

depicted in Fig. 1 and the cracked behaviour of the tubular specimen is indicated in Fig. 2.

3.1. Uncracked phase

During a first-time loading, the behaviour is linear elastic in the initial phase, when the applied moment is less than the so-called 'cracking moment', M_r (Fig. 1). The 'cracking moment' may be defined as that value of the applied moment which results in the maximum tensile stress (at point B in Fig. 2c) reaching the tensile strength[1] (f_{ct}) of concrete. During this initial phase (path 'Oa' in Fig. 1), the tubular section is assumed to be uncracked and the slope of the M-φ line in this region is constant, and equal to the uncracked flexural rigidity (EI_{uc}) of the tubular section. This is easily obtainable as the product of the short-term elastic modulus of concrete (E) and the second moment of area (I_{uc}) corresponding to the gross transformed (annular ring) section, given by :

$$I_{uc} = \pi r^3 t\,(1+p\tilde{m}/100) \tag{1}$$

[1] Note that it is more appropriate to consider the *direct tensile strength* (f_{ct}) rather than the *modulus of rupture* (f_{cr}), as the shape of the large hollow circular section is such that the distribution of tensile stress across the thickness of the concrete shell is practically uniform (Menon 1994).

where r and t denote the mean radius of the tower section and thickness of the concrete shell, respectively (Fig. 2); p denotes the percentage steel (in terms of area of steel with respect to gross area of the section); and $\tilde{m}$ denotes the 'modular ratio' (i.e., ratio of elastic modulus of steel to that of concrete).

The cracking moment (M_r) is obtainable from the stress relation:

$$f_{ct} = \frac{M_r}{I_{uc}/r} - \frac{N}{2\pi rt\,(1+p\tilde{m}/100)}$$

whereby

$$M_r = f_{ct} \cdot \pi r 2t\,(1+p\tilde{m}/100)+Nr/2 \tag{2}$$

It is noteworthy that the cracking moment depends not only on the material and cross-sectional properties, but also on the magnitude of normal compression (N).

3.2. Cracked phase

When, in a beam segment subjected to a constant moment, the moment crosses M_r, the concrete in tension is (theoretically) expected to crack and fail throughout the length of the specimen at the maximum stress location (point 'B' in Fig. 2c), with the cracks propagating towards the neutral axis. However, in reality, cracking occurs at discrete and randomly spaced locations along the length of the beam segment such that significant portions, in between cracks, remain uncracked (Fig. 2a). The concrete, in between the cracks, resists some tension, and this is reflected by variations in the neutral axis (Fig. 2a), bond stress, and tensile strain in the reinforcing steel (Fig. 2b). Whereas, for the purpose of designing the steel reinforcement, it is appropriate to consider the section to be cracked, it would be unrealistic to assume *all* sections along the beam length to be cracked for the purpose of deflection calculations. The tensile strain midway between the cracks (at the section marked ② in Fig. 2) may be as low as 60 percent of the strain at the crack location (marked ①). As the applied moment increases, the cracking becomes more widespread, and the difference between the two strains gets reduced, and eventually gets almost eliminated as limit state conditions are approached (Pillai and Menon 1998).

The moment-curvature relationship in the cracked phase is nonlinear (Fig. 1), and the flexural rigidity corresponding to any moment (M), is obtainable as the secant modulus, which reduces with increasing moment on account of increased cracking. The curvature (φ) in the cracked phase, corresponding to a moment (M) on the beam segment (subjected to constant bending moment), is obtainable from the strain profiles at various sections of the beam. As shown in Fig. 2c, the strain profile at the crack location (section ①) is different from that at the section midway between cracks (section ②). From theoretical analysis, we can estimate the extreme strains in compression (ε_c) and tension (ε_s) at the cracked section ①, such that the corresponding stresses result in a bending moment equal to the applied moment (M). The curvature calculated on the basis of these strains (Fig. 2c) may termed 'cracked curvature' (φ_{cr}) and is easily obtainable as :

$$\varphi_{cr} = \frac{\varepsilon_c + \varepsilon_s}{2r} \tag{3}$$

It is not possible, except with the help of additional simplifying assumptions, to predict theoretically the variation of the strain profile, and hence the variation of the curvature, in the beam segment between two cracks. Clearly, the actual curvature of the total beam, subjected to a constant moment (coupled with a constant axial compression), is related to some *mean strain profile* (Fig. 2c). Such a curvature, called 'effective curvature' (φ_{eff}) may be related to the 'cracked curvature' (φ_{cr}) as follows :

$$\varphi_{eff} = \lambda \cdot \varphi_{cr} \tag{4}$$

where λ is a coefficient, having a value less than unity. The two nonlinear moment-curvature relationships in the cracked phase, viz., M-φ_{eff} and M-φ_{cr}, are depicted schematically in Fig. 1, the former by means of a solid line and the latter by means of a dashed line.

3.3. Tension stiffening effect

Deflection calculations in RC beams are sometimes based, for sheer convenience, on the flexural rigidity of the gross (uncracked) section. Such an assumption has the advantage of extreme simplicity, but will clearly result in underestimated values of deflections, especially under relatively high moments. It is possible, with some computational effort, to estimate the 'cracked curvature' (φ_{cr}), using Eq. (3), and hence arrive at the so-called 'cracked flexural rigidity' ($EI_{cr} = M/\varphi_{cr}$), corresponding to any given moment (M). However, deflection calculations based on EI_{cr} are likely to be overestimated, because such calculations implicitly assume that all sections of the beam are fully cracked on the tension side of an invariant neutral axis location.

In order to arrive at a more realistic prediction of deflections (for even simple cases involving 'pure bending'), it is necessary to account properly for the discrete and variable nature of the cracking phenomenon, by considering the M-φ_{eff} relationship in Fig. 1 (instead of the M-φ_{cr} curve). The secant modulus obtainable from the M-φ_{eff} plot (as the slope of the line 'Ob' in Fig. 1) is termed the 'effective flexural rigidity' ($EI_{eff} = M/\varphi_{eff}$). Typically, it has a value which is less than the cracked flexural rigidity, but greater than the uncracked flexural rigidity (Fig. 1). The increase in stiffness (over the cracked stiffness), on account of consideration of the tension in the concrete in between cracks, is termed *tension stiffening*.

The coefficient λ in Eq. (4) accounts for this tension stiffening effect, and hence may be appropriately termed 'tension stiffening factor'. The value of this factor depends on the applied moment (M), the reinforcement percentage (p), and also the magnitude of the axial compression (N). The problem that now remains is to develop a suitable formula for λ in terms of these three basic variables, ideally on the basis of experimental test results.

4. Proposed empirical formula for tension stiffening factor

A functional description of the 'tension stiffening factor' ($\lambda \equiv \varphi_{eff}/\varphi_{cr}$) is proposed in this paper, on an analysis of the experimental results reported by Schlaich *et al* 1979. The test data, in terms of measurements of moment-curvature, pertain to RC tubular specimens, each with a length of 6 m, outer diameter of 1.2 m, and shell thickness of 100 mm, subjected to combined bending and axial compression. The tests were carried out, with the tubes placed horizontally and simply supported at the two ends. Axial compressive forces were introduced by means of centrally located prestressed tendons, and were maintained at a constant level throughout the test duration. Moments of equal magnitude were applied at the two ends of the

tubes to cause bending in single curvature, and were increased in stages till failure occurred. The tubes differed mainly in the reinforcement percentages (0.454, 0.818 and 1.636) and the normal compression levels[2] (0 kN, 1000 kN and 2000 kN). The concrete used had a grade (characteristic cube strength) of 25 MPa. Some typical test results are depicted in the moment-curvature plots shown in Fig. 3.

For the purpose of developing an empirical formula for the dimensionless factor λ, it is desirable, in the interest of generalisation, to resort to nondimensionalised basic variables. Thus, instead of bending moment (M), and normal compression (N), the following normalised parameters are used in the present formulation :

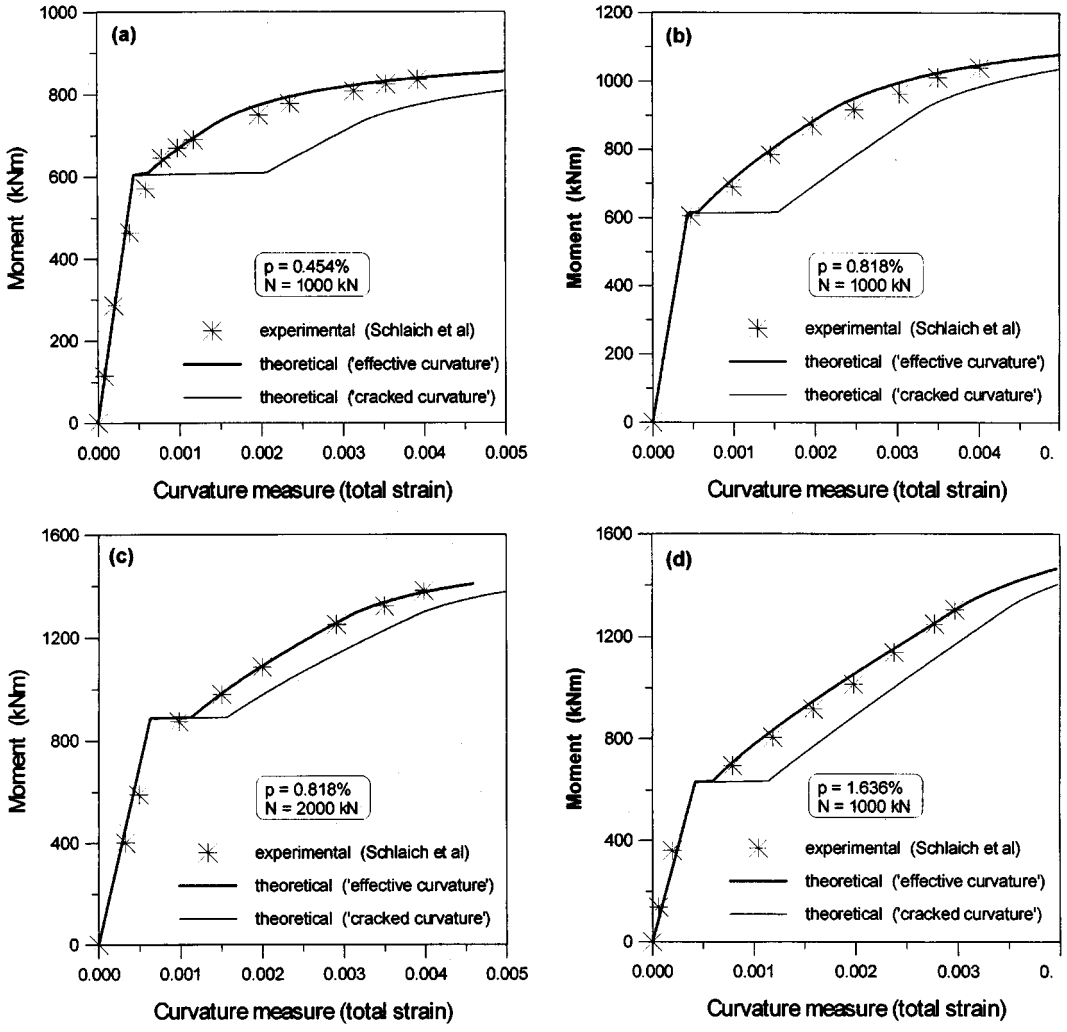

Fig. 3 Moment-curvature relationships – experimental and theoretical

[2] As the axial compression levels are very small in comparison with the critical buckling load, the second-order effects (due to beam-column behaviour) on the moment-curvature relationship are negligible.

$$\mu \equiv M/M_{cr} \tag{5}$$

$$n \equiv N/f_{ck}\, rt \tag{6}$$

where f_{ck} is the characteristic cube strength of concrete, and the other variables are as described earlier. We now seek an empirical formula for λ in terms of μ, p and n.

For given values of p and n, it is seen from an analysis of the test data that there is a somewhat parabolic variation of λ with respect to μ. Similar trends are seen in the variations of λ with p and with n. Through a process of multiple Lagrangian interpolation, the following formula for λ in terms of μ, p and n is generated :

For $\mu > 1.0$,

$$\lambda = (6-5\mu+\mu^2)(0.955-0.306p+0.442p^2)(0.220-0.221n+0.205n^2) - (9.267+13.476\mu-4.209\mu^2) \tag{7}$$

Although the formula appears to be rather lengthy, it is found to generate moment-curvature relationships that are in good agreement with the test results. Some typical results are depicted graphically in Fig. 3; the graphs include the test data, and the M-φ_{cr} and M-φ_{eff} curves obtained theoretically. The M-φ_{cr} plots are generated by an analysis of the RC tubular section with appropriate assumptions (Menon 1994) and stress-strain curve models for concrete and steel (Rao and Menon 1995). The location of the neutral axis and the extreme strains ε_c and ε_s (in Fig. 2c) are obtained through a numerical scheme, in which the governing equations (involving M and N) are formed from force and moment equilibrium considerations. After generating the 'cracked curvature' (φ_{cr}) for given values of M and N, and determining the appropriate value of the 'tension stiffening factor' (λ) using Eq. (7), the 'effective curvature' (φ_{eff}) is determined by applying Eq. (4); thus, the M-φ_{eff} plots are generated. It may be noted that in the graphs shown in Fig. 3, a dimensionless measure of curvature, $\varphi \cdot 2r$, is used for the abscissas. This 'curvature measure' is, incidentally, equal to the sum of the extreme strains ('total strain') at points A and B in Fig. 2c. In the case of the 'cracked curvature' plot, it is equal to ($\varepsilon_c+\varepsilon_s$), whereas in the case of the 'effective curvature' plot, it is equal to the 'total strain' corresponding to some mean strain profile.

4.1. Influences of reinforcement percentage and axial compression

The influences of the reinforcement percentage (p) and the axial (normal) compression parameter (n) on the moment-curvature relationship, using the proposed formulation, are typically as depicted in Fig. 4a and Fig. 4b respectively. For convenience, the ordinate (moment) is nondimensionalised in terms of a 'moment parameter' (m), which is similar to the normal compression parameter (n), and is commonly used in m-n interaction diagrams (Rao and Menon 1995) :

$$m \equiv M/(f_{ck}\, r^2 t) \tag{8}$$

The following inferences may be drawn from the graphs shown in Fig. 4 :

- The flexural rigidity in the uncracked phase does not increase appreciably with increase in reinforcement; hence, considering the gross concrete section, rather than the uncracked transformed section, in the uncracked (linear elastic) phase, is a simplification (often adopted in practice) which is reasonable.
- The linear elastic phase gets extended with increase in normal compression, on account of increase in the magnitude of cracking moment; however, flexural rigidity remains

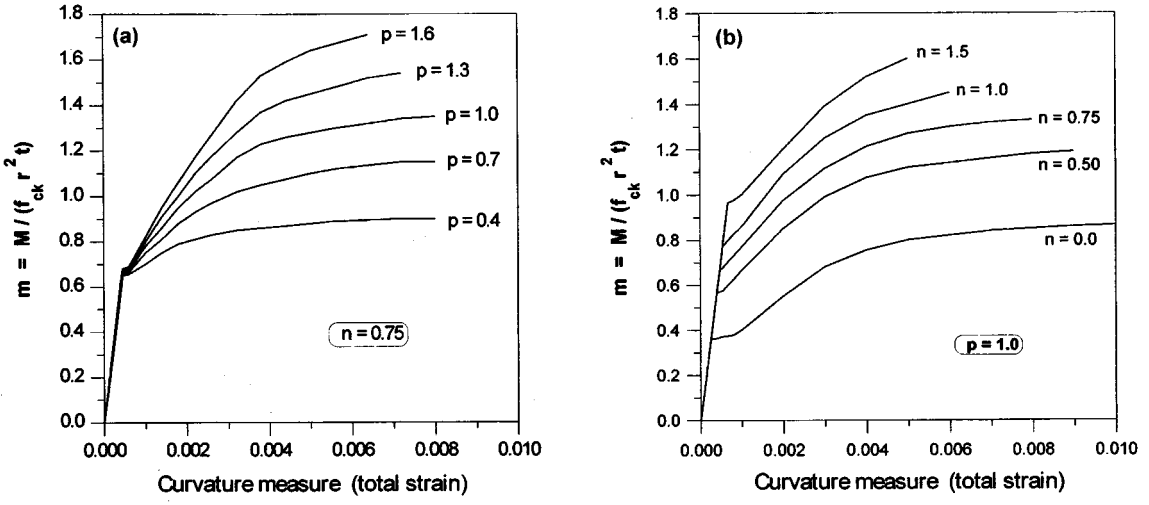

Fig. 4 Influences of (a) reinforcement percentage and (b) axial compression on Moment-curvature relationship

completely unaffected.

- In the post-cracking phase, flexural rigidity increases with increase in reinforcement, as well as increase in normal compression.
- Ductility in the post-cracking phase decreases with increase in normal compression, on account of reduction in the extreme steel strain at the limit state; in the case of a 'compression failure' (rather than the more common 'tension failure'), it is likely that the extreme tension steel may not have yielded at all.

5. Determination of deflections and second-order moments

In the preceding sections, the problem of estimating flexural rigidity (EI) of an RC tubular tower segment, subjected to uniform bending moment (M) and normal compression (N), has been addressed. When the moment is less than the 'cracking moment' (M_r), given by Eq. (2), the flexural rigidity of the gross uncracked section (EI_{uc}) is applicable. Otherwise (when $M > M_r$), the effective flexural rigidity (EI_{eff}), which accounts for the variable and discrete nature of cracking, has to be determined; a detailed procedure for this has been presented in this paper.

In the practical case of the wind-loaded tower, the distribution of bending moments, as well as that of normal compression along the height of the tower, is nonuniform, with the maximum values of M and N located at the base. Every section along the height of the tower is subjected to a unique combination of M and N, with the consequence that the distribution of flexural rigidity is nonuniform along the height of the tower. The upper region of the tower may remain uncracked, on account of low bending moments in this region.

In conventional RC beams, with nonuniform bending moment diagrams, simplified formulae have been devised to enable the designer to make use of a single value of (EI_{eff}) for the entire beam, in association with the maximum moment, to estimate the maximum short-term deflection in the beam (ACI 318, 1989, BS 8110, 1985). However, it is assumed in such cases that the beam is prismatic (i.e., has the same gross cross-section throughout the span). Simplified formulae, with a similar basis, have been proposed by Naokowski 1981 and CICIND 1984 to facilitate the determination of second-order moments in wind-loaded RC chimneys; the underlying assumption

is that the chimneys are *cylindrical* in cross-section. It is doubtful whether such simplified formulae can be reasonably applied to the more general and practical case of *tapered* chimneys and towers. It may be noted that the procedure described in this paper, although somewhat rigorous (because it involves determination of flexural rigidity at frequent intervals along the height of the tower), is applicable to *all* tower profiles.

Another issue that needs to be addressed is that the theoretical moment-curvature relationships, such as the one depicted in Fig. 1, are strictly applicable only for 'first-time loading' situations. When an RC flexural member has been subjected previously to a higher moment level than the present one under consideration, then the degree of cracking, and consequent effective flexural rigidity, will be governed by that previous higher moment (whose magnitude may not be known)! In the context of 'strength design' of wind-loaded RC towers, we are interested in the deflections and consequent second-order moments that are liable to be induced by an *extreme* wind (with a definite acceptable risk of exceedance). In such a situation, it is reasonable to consider this extreme wind loading as an instance of 'first-time loading', as no cross-section of the tower (designed as a vertical cantilever) is expected (from a design point-of-view) to have a resistance beyond this theoretical limit state. However, if deflections are sought under a lesser wind load (as under the 'so-called serviceability limit state'), then calculations based on flexural rigidities induced by the extreme wind will be conservative.

5.1. Proposed procedure

A truly rigorous procedure for determining the response of wind-loaded towers calls for a nonlinear stochastic dynamic analysis, which is computationally too intensive to find acceptance in design practice. The proposed procedure recognises this, and merely attempts to modify the prevailing codal design practice to include second-order effects.

In the conventional procedure for estimating along-wind moments in RC chimneys and towers, a static analysis is first performed to determine the 'primary' (first-order) moments that arise due to a *mean* wind load profile. These moments are then multiplied by appropriate gust factors, which account for the dynamic amplification effect (Menon and Rao 1997a) :

$$M_z = G_z \cdot M_{mz} \tag{9}$$

In the above equation, M_z, M_{mz} and G_z denote, respectively, the peak moment, the mean moment and the gust factor at a height z above the ground level. In 'strength design' procedures, the peak moment (M_z) is further magnified by an appropriate 'wind load factor' to account for the enhancement in response under an extreme wind. This factor supposedly also accounts for the nonlinear increase in gust factor, under very high wind velocities (Kaemmer *et al*, 1989, Menon 1994).

In the proposed procedure, the first-order deflections (corresponding to the 'primary', moments) are first determined based on a linear finite element analysis, using simple beam elements to model the vertical shaft (Menon and Reddy 1998). For this purpose, the gross (uncracked) sectional properties are considered while assembling the global stiffness matrix. An initial estimate of the second-order moments is then arrived at, by evaluating the P-Δ effects at the various nodes along the shaft height, on account of the dead loads acting at the various levels. The sum of the primary moment and the second-order moment at any node gives the total

moment; corresponding to the total moments at various sections, the appropriate flexural rigidities are evaluated using the moment-curvature relationships discussed earlier in this paper. The global stiffness matrix is revised accordingly, and the deflections and second-order moments recalculated. This process of step-wise linear analysis is iterated until satisfactory convergence of results is attained; the tip deflection or the base moment can be used as the parameter on which convergence is based.

5.2. Example application

The application of the proposed procedure to a linearly tapered RC chimney (Menon 1994) is given here. The example tower has a height $h = 200$ m; a base (outer) diameter $D_b = 20$ m; a top diameter $D_t = 12$ m, a concrete shell thickness of 575 mm at base, tapering linearly to 250 mm at top; a uniform reinforcement percentage p=1.0; and a concrete grade $f_{ck} = 25$ MPa. The tower is assumed to be located in open country terrain with a mean hourly wind speed $V_{10} = 37.5$ m/s at a height of 10 m above ground.

The results are depicted graphically in Fig. 5. It is seen that deflections (Fig. 5a) and second-order moments (Fig. 5b) are grossly underestimated when based on uncracked section properties (as is sometimes done in practice). Further, it is seen from Fig. 5c that, whereas first-order (primary) moments (M_p) increase highly nonlinearly at sections further removed from the top of the tower (due to cantilever action), the second-order moments (M_s) show such an increase only up to about one-fourth of the height above the base ($z > 0.25h$). In the lower one-fourth region ($z < 0.25h$), the increase in second-order moments is marginal, because the deflections in this region are extremely small (nearly zero), due to the assumed fixity at the base. Consequently, the ratio of the second-order moment to the first-order

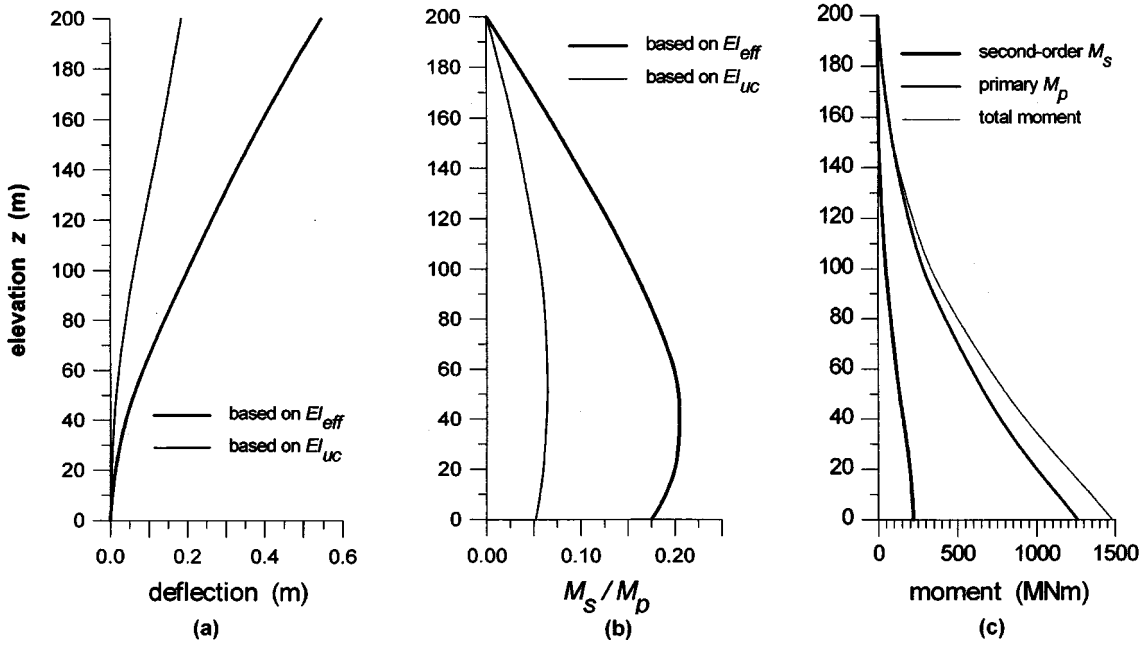

Fig. 5 Example tower – (a) deflection profile, (b) M_s/M_p profile, and (c) moment profiles

moment (M_s/M_p) is found to be maximum at $z \approx 0.25h$, and in this example is as high as 21 percent (Fig. 5b).

5.3. Influences of wind speed, tower slenderness and height

It is expected that, under extreme wind conditions, the mean wind speed (V_{10}) will increase beyond the specified reference speed V_R (usually having a return period of 50 years), and under ultimate load conditions, may take a value as high as 1.25 V_R. For the 200 m tower studied earlier, considering $V_R = 30$ m/s, it is seen from the results depicted in Fig. 6a, that the maximum M_s/M_p ratio (at $z \approx 0.25h$) increases from 0.10 (for $V_{10}/V_R = 1.0$; i.e., 'service load' condition) to 0.21 (for $V_{10}/V_R = 1.25$; i.e., 'ultimate load' condition).

The height-base diameter ratio (h/D_b) may vary in the range 7 to 13 in design practice, the lower values being resorted to usually in multiflue chimneys. High h/D_b ratios are indicative of slender towers, and in such cases, second-order moments are likely to be significant. The results of a parametric analysis (Fig. 6b) indicate that the maximum M_s/M_p ratio increases from 3 percent (for h/D_b=7) to as much as 35 percent (for h/D_b=13), for the example tower discussed earlier. Second-order moments appear to be significant (more than 10 percent of the primary moments) when the slenderness ratio (h/D_b) exceeds about 9.

The influence of tower height (h) on second-order effects is depicted in Fig. 7. As expected, the deflections (Fig. 7a) and second-order moments (Fig. 7b) increase with increasing height. However, it is interesting to observe that whereas the tip deflection-height ratio remains almost the same for all heights (given the same V_{10} and h/D_b), the maximum M_s/M_p ratio increases significantly from 7 percent (for $h = 100$ m) to 30 percent (for $h = 300$ m). Second-order moments may be considered to be significant when the height of the tower exceeds about 150 m.

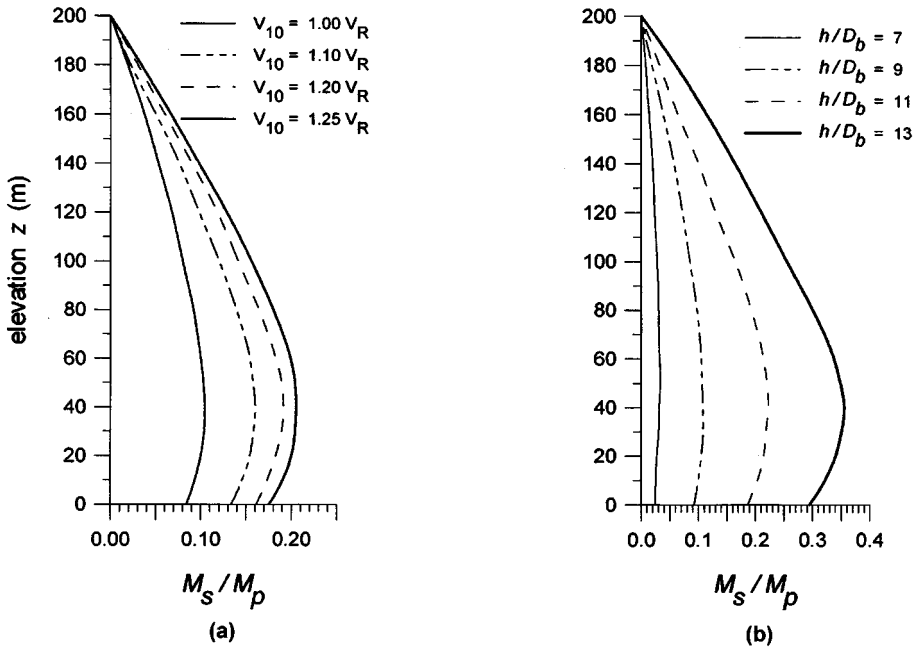

Fig. 6 Influences of (a) wind speed and (b) tower slenderness on second-order moments

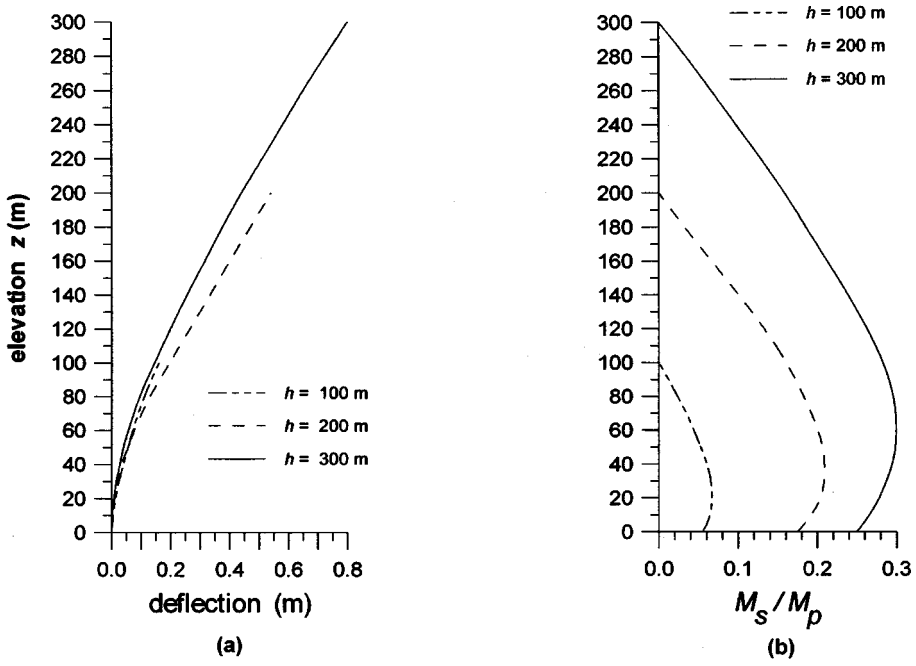

Fig. 7 Influence of tower height on (a) deflection profile and (b) M_s/M_p profile

6. Conclusions

1. An empirical formula [Eq. (7)] is proposed to enable the prediction of the 'effective curvature' [Eq. (4)] in RC towers of tubular cross-section, subject to bending (due to lateral wind loading) combined with axial compression (due to dead load). The proposed formula, based on the experimental work of Schlaich *et al* 1979 and theoretical formulation of Menon 1994, accounts for the effects of variable cracking and tension stiffening in concrete.

2. Moment-curvature relationships, based on the proposed formula, account for the increase in flexural rigidity with increase in reinforcement percentage and increase in axial compression (Figs. 4a, 4b).

3. Using the proposed moment-curvature relationships, it is shown how a nonlinear quasi-static analysis (including second-order effects) may be performed to determine the deflections and moments along the height of the wind-loaded tower. It is demonstrated, by means of an example, that second-order moments of significant magnitude can develop in the tower, and that these moments can be grossly underestimated when calculations are based on the uncracked sectional properties (as is sometimes done in practice). It is also observed that the maximum increase in moment (due to second-order effects) over the primary moment occurs, not at the base of the tower, but at approximately one-fourth the height of the tower.

4. By means of a parametric study, it is indicated that second-order moments become too significant to be ignored in design when the wind speed is high (as, under ultimate load conditions), when the tower is relatively slender ($h/D_b > 9$), and when the tower is relatively tall ($h > 150$ m).

7. Closure

Most codes on RC chimney design have not yet incorporated provisions for the explicit determination of second-order moments, essentially because of the difficulties associated with the prediction of the moment-curvature relationships, due to variable cracking and tension stiffening in concrete. It is hoped that the work reported here will serve as a research contribution in this area.

References

ACI 318R (1989). Commentary on Building Code Requirements for Reinforced Concrete ACI 318-89, American Concrete Institute, Detroit, Michigan.

ACI 307 (1988). Standard Practice for the Design and Construction of Cast-in-place Reinforced Concrete Chimneys (ACI 307-88) and Commentary (ACI 307R-88), American Concrete Institute, Detroit, Michigan.

Beeby, A.W. and Miles, J.R. (1969), "Proposals for the control of deflection in the new unified code", *Concrete*, **3**(3), 101-110.

Branson, D.E. (1977). *Deformation of Concrete Structures*, McGraw-Hill Inc., New York.

BS 8110 (1985). "Structural use of concrete : Part 2 : Code of practice for special circumstances", British Standards Institution, London.

CICIND (1984). "Model code for concrete chimneys – Part A : The shell", Comité International des Chimnees Industrielle, Zurich.

DIN 1056 (1984). "Solid construction, free-standing stacks : Calculation and design", Deutsches Institut fur Normung, Germany.

IS 4998 (1992). "Indian standard practice for design of reinforced concrete chimneys : Part I : Design criteria (First Revision)", Bureau of Indian Standards, New Delhi.

Kaemmer, K., Schueller, G.I. and Pradlwarter, H.J. (1989), "Influence of nonlinearities in oscillations on along-wind gust response of RC chimneys", *Engineering Structures*, **11**, 69-74.

Menon, D. (1994). "Reliability of wind-resistant design of tubular RC towers", PhD Thesis, Dept of Civil Engrg, Indian Institute of Technology, Madras.

Menon, D. and Rao, P.S. (1997a), "Estimation of along-wind moments in RC chimneys", *Engineering Structures*, **19**(1), 71-78.

Menon, D. and Rao, P.S. (1997b), "Uncertainties in codal recommendations for across-wind load analysis of RC chimneys", *J. Wind Engrg and Industrial Aerodynamics*, **72**(3), 455-468.

Menon, D. and Rao, P.S. (1998), "Reliability of wind-resistant design of tubular reinforced concrete towers", *J. Struct. Engrg*, SERC, **25**(4), 21-29.

Menon, D. and Reddy, Y.N. (1998), "Finite element modelling of tall slender tubular towers", *J. Struct. Engrg*, SERC, **24**(1), 243-246.

Mokrin, Z.A.R. and Rumman, W.S. (1985), "Ultimate capacity of reinforced concrete members of hollow circular sections subjected to monotonic and cyclic bending", *ACI Journal*, **82**, 653-656.

Naokowski, P. (1981), "Simplified determination of the moments of second-order in industrial chimneys", *Proceedings of the Fourth International Symposium on Industrial Chimneys*, The Hague, Netherlands, May.

Naokowski, P. and Gerstle, K.H. (1990), "Tower structures subjected to temperature and wind", *ACI Structural Journal*, **87**(4), 479-487.

Pillai, S.U. and Menon, D. (1998). *Reinforced Concrete Design*, Tata McGraw-Hill, New Delhi, 333-374.

Pinfold, G.M. (1984). *Reinforced Concrete Chimneys and Towers*, Viewpoint Publication, second edition.

Prakhya, G.K.V., and Morely, C.T. (1990), "Tension stiffening and moment-curvature relations of reinforced concrete elements", *ACI Structural Journal*, **87**(9), 597-602.

Rao, P.S. and Subrahmanyam, B.V. (1973), "Trisegmental moment-curvature relations for reinforced concrete members", *ACI Journal*, **70**(5), 346-352.
Rao, P.S and Menon, D. (1995), "Ultimate strength of tubular RC tower sections under wind loading", *Indian Concrete Journal*, **69**(2), 117-123.
Sakai, K. and Kakuta, Y. (1980), "Moment-curvature relationships of reinforced concrete members subjected to combined bending and axial force", *ACI Journal*, **77**(5), 189-194.
Schlaich, J., Schober, H. and Koch, R. (1979). Versuche zur Mitwirkung des Betons in der Zug-zone von Stahlbetonrohren, Bericht des Instituts für Massivbau der Univeristat Stuttgart.
Yu, W.W., and Winter, G. (1960), "Instantaneous and long-time deflections of reinforced concrete beams under working loads", *ACI Journal*, **57**(1), 29-50.

(Communicated by Chang-Koon Choi)